

# Stable, High-Molecular-Weight Poly(phthalaldehyde)

Jared M. Schwartz, Oluwadamilola Phillips, Anthony Engler, Alexandra Sutlief, Jihyun Lee, Paul A. Kohl

School of Chemical and Biomolecular Engineering, Georgia Institute of Technology, Atlanta, Georgia 30332-0100

Correspondence to: P. A. Kohl (E-mail: kohl@gatech.edu)

Received 19 October 2016; accepted 8 November 2016; published online in Wiley Online Library

DOI: 10.1002/pola.28473

**ABSTRACT:** Low ceiling temperature, thermodynamically unstable polymers have been troublesome to synthesize and keep stable during storage. In this study, stable poly(phthalaldehyde) has been synthesized with  $\text{BF}_3\text{-OEt}_2$  catalyst. The role of  $\text{BF}_3$  in the polymerization is described. The interaction of  $\text{BF}_3$  with the monomer is described and used to maximize the yield and molecular weight of poly(phthalaldehyde). Various Lewis acids were used to investigate the effect of catalyst acidity on poly(phthalaldehyde) chain growth. *In situ* nuclear magnetic resonance was used to identify possible interactions formed between  $\text{BF}_3$  and phthalaldehyde monomer and polymer. The

molecular weight of the polymer tracks with polymerization yield. The ambient temperature stability of poly(phthalaldehyde) was investigated and the storage life of the polymer has been improved. © 2016 Wiley Periodicals, Inc. *J. Polym. Sci., Part A: Polym. Chem.* **2016**, *55*, 1166–1172

**KEYWORDS:** accelerated aging; boron trifluoride; cationic polymerization; complexation; *in situ* NMR; nonlinear polymers; phthalaldehyde; polyaldehyde; self-immolative; stability; stimuli-sensitive polymers; transient

Thermodynamically unstable polymers have emerged in applications where a catalytic response to a small trigger is necessary or environmental degradation is desired.<sup>1–4</sup> The amplified degradation in macro-scale plastics offers a solution to a variety of problems including drug delivery, dry-developing photoresists, and transient electronics.<sup>4–11</sup> The catalytic response to a stimulus allows the polymer to efficiently and rapidly decompose into its original monomer or other small molecule products.

Poly(phthalaldehyde) (PPHA) is highly sensitive to acid and has been shown to rapidly depolymerize when deprotected either by end-group removal or direct chain attack.<sup>12,13</sup> The polymerization of phthalaldehyde (PHA) can proceed by either an anionic or cationic mechanism.<sup>11,12,14,15</sup> The anionic mechanism allows control over the end groups of the polymer chain (i.e., potential trigger sites), while the cationic mechanism provides a more thermally stable polymer.<sup>12,15</sup> Two issues have plagued the polymerization of PHA, namely the reproducibility of the polymerization in achieving high molecular weight and the long term shelf-life of the polymer.<sup>6,16</sup> A high molecular weight is desired for creating thick polymer films because chain entanglement provides mechanical strength.

One promising pathway for achieving high molecular weight is through the cationic synthesis route utilizing boron trifluoride etherate ( $\text{BF}_3\text{-OEt}_2$ ) catalyst.<sup>7,14,15,17,18</sup>

Kaitz et al. found that the  $\text{BF}_3\text{-OEt}_2$  catalyst forms a cyclic polymer with high thermal stability.<sup>15</sup> Previous studies with  $\text{BF}_3\text{-OEt}_2$  catalyst support the concept that a cationic chain end is produced from a Lewis acid.<sup>15,19</sup> This cationic end is free to propagate the polymer chain. No evidence of the counter-ion produced to stabilize this propagating chain was provided.<sup>15,19,20</sup> Reported values of yield, molecular weight, and polydispersity index for PPHA suggest that cationic addition chain propagation is unlikely.

This article seeks to identify the participation of  $\text{BF}_3\text{-OEt}_2$  in the polymerization of PHA, specifically in the interaction of  $\text{BF}_3$  with the monomer. A possible mechanism is proposed to help explain the phenomenon observed in the experiments presented here as well as those previously reported. Strong evidence for a unique role of  $\text{BF}_3$  in the polymerization of PHA is presented.

Stability has also been called into question when working with polyaldehydes.<sup>6</sup> The experience of the authors is that there is sudden depolymerization of the polymer even after weeks of what appears to be a stable material. In attempting to unravel the role of  $\text{BF}_3$  in the polymerization of PHA, a method for improving the polymer stability after polymerization was discovered. A procedure for increasing the shelf-life of PPHA is also reported.

© 2016 Wiley Periodicals, Inc.

**TABLE 1** List of Lewis Acid Catalysts for PPHA Polymerization

Lewis Acid	Polymer Yield	Acidity <sup>a</sup>
ZnCl <sub>2</sub>	–	1.70
AlEt <sub>3</sub>	–	N/A <sup>b</sup>
BF <sub>3</sub> -OEt <sub>2</sub>	80.2%	2.76
TiF <sub>4</sub>	–	2.78
TiCl <sub>4</sub>	30.0%	2.93
BCl <sub>3</sub>	–	4.08
BBr <sub>3</sub>	–	4.33

<sup>a</sup> Relative acidities from Hilt et al.<sup>23</sup>

<sup>b</sup> Relative acidity value of AlEt<sub>3</sub> not reported.

Catalysts are listed in ascending order of acidity.

## EXPERIMENTAL

### Materials

Ortho-PHA was obtained from Alfa Aesar (98% purity) and purified by sublimation in a nitrogen rich atmosphere at 45°C. BF<sub>3</sub>-OEt<sub>2</sub> (ca., 48% BF<sub>3</sub>) and titanium (IV) tetrafluoride (TiF<sub>4</sub>) were purchased from Acros Organics and used as-received. ACS Reagent-grade hexane, tetrahydrofuran (THF), and methanol were purchased from BDH and used as-received. ACS Reagent-grade dichloromethane (DCM) and diethyl ether were purchased from BDH and dried over 3 Å molecular sieves. Deuterated DCM (CD<sub>2</sub>Cl<sub>2</sub>), boron trichloride (BCl<sub>3</sub>), and boron tribromide (BBr<sub>3</sub>) were purchased from Sigma-Aldrich and used as-received. Titanium (IV) tetrachloride (TiCl<sub>4</sub>) and triethylaluminum (AlEt<sub>3</sub>) were purchased from Alfa Aesar. Triethylamine (TEA) was purchased from AMRESCO and used as-received. Zinc (II) chloride was purchased from J.T. Baker and treated with thionyl chloride to remove water. Hexafluorobenzene (99% purity) was purchased from TCI America and used as-received.

### Methods

For the polymerizations, 2 g (15 mmol) of PHA monomer was dissolved in 20 mL DCM in a 100 mL round bottom flask in a nitrogen purged glovebox. To the monomer solution, a catalyst was added and the flask sealed with a septum. The flask was cooled to –78°C and allowed to react for

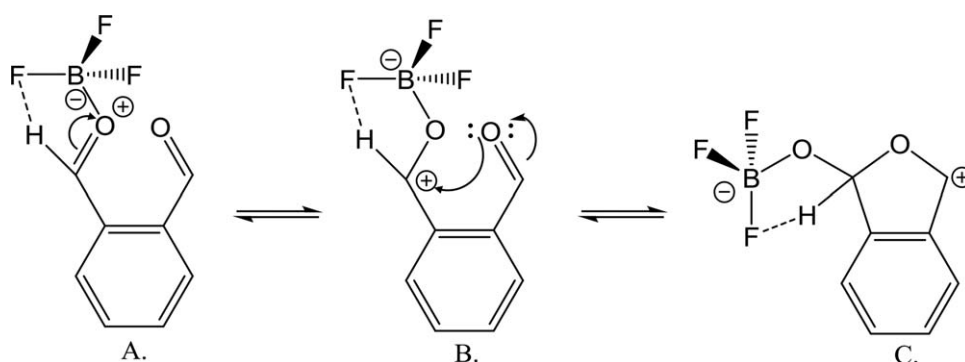
the desired length of time. The reaction was quenched with 0.24 mL (3 mmol) pyridine. The subsequent solution was precipitated into methanol and filtered. The precipitate was redissolved in either THF or DCM; 0.05 mL (0.36 mmol) of TEA per gram of precipitate was added to some polymers to help remove residual catalyst. The polymer in either THF or DCM was precipitated into hexane, filtered, and allowed to dry until constant weight was achieved.

*In situ* <sup>1</sup>H and <sup>19</sup>F nuclear magnetic resonance (NMR) in CD<sub>2</sub>Cl<sub>2</sub> was performed in a Bruker Avance III 400 MHz tool. Temperature was calibrated by the relation of the chemical shift differences of a pure solution of methanol.<sup>21</sup> Molecular weight and *D* were determined by gel permeation chromatography (GPC) in a Shimadzu GPC tool equipped with an LC-20 AD HPLC pump and a refractive index detector (RID-10 A, 120 V). THF was used as the eluent with a flow rate of 1.0 mL/min at 35°C. The molecular weight was measured by a calibration curve based on polystyrene standards. Accelerated aging was performed in a TA Instruments Thermal Gravimetric Analysis (TGA) Q50 with a ramp rate of 20°C/min to 10°C below desired isothermal temperature and a 1°C/min ramp over the remaining 10°C to the final temperature to avoid overshoot. A N<sub>2</sub> rich atmosphere with a flow rate of 40 mL/min was used.

## RESULTS AND DISCUSSION

To test the effect of Lewis acidity on PPHA chain growth, various Lewis acids were used as the catalyst in the polymerization.<sup>22</sup> Lewis acids were chosen to span a wide range of acidities. The same catalyst loading, 0.03 mmol, was used for all polymerizations. The acids, presented in increasing acidity, were ZnCl<sub>2</sub>, AlEt<sub>3</sub>, BF<sub>3</sub>-OEt<sub>2</sub>, TiF<sub>4</sub>, TiCl<sub>4</sub>, BCl<sub>3</sub>, and BBr<sub>3</sub>.<sup>23–25</sup> Table 1 shows polymer yields and relative acidities for the Lewis acids used.<sup>23</sup> Only two Lewis acids produced polymer under these conditions: BF<sub>3</sub>-OEt<sub>2</sub> and TiCl<sub>4</sub>.

Interestingly, the only borohalide to produce polymer was BF<sub>3</sub>-OEt<sub>2</sub>. Other borohalides were used in an attempt to determine the effect of a decrease in hydrogen bonding to halide, in the order of F > Cl > Br.<sup>26</sup> In any condition where BF<sub>3</sub> was not used, no yield was obtained despite a color



**SCHEME 1** Proposed initiation mechanism of BF<sub>3</sub> and PHA with the initial complexation (A), rearrangement of the cation to the formyl carbon (B), and the cyclized monomer cation (C).

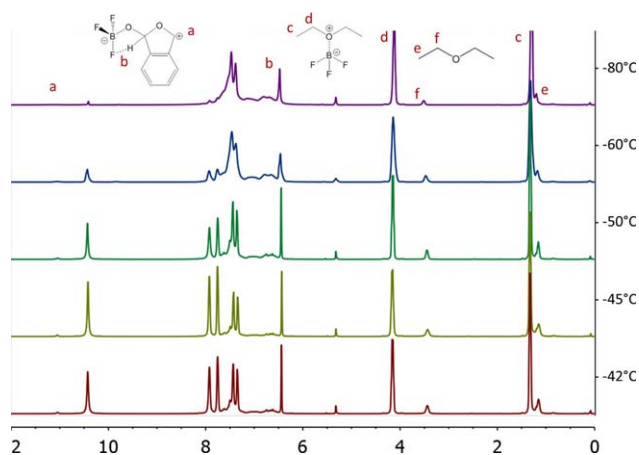


**FIGURE 1** *In situ*  $^1\text{H}$  NMR spectra of PHA polymerization in  $\text{CD}_2\text{Cl}_2$  with  $\text{BF}_3\text{-OEt}_2$  as the initiator. [Color figure can be viewed at [wileyonlinelibrary.com](http://wileyonlinelibrary.com)]

change being observed on addition of the borohalide.  $\text{BF}_3$  clearly has a unique interaction with the PHA monomer. One explanation is that the conformational configuration of  $\text{BF}_3$  supports a cationic propagating chain. The formyl proton interacts with a  $\text{BF}_3$  fluorine forming a complex at closer than the summation of their van der Waals radii as shown in Scheme 1(A).<sup>26</sup> This  $\text{BF}_3\text{-H}$  complex shifts the cationic site from the boron-oxygen to the formyl carbon, Scheme 1(B). This allows cationic propagation through a cation-aldehyde interaction, Scheme 1(C).

Some papers suggest a co-initiator is necessary for borohalides, although these papers focus on the polymerization of olefins.<sup>27,28</sup> Diethyl ether was added to a solution of DCM and either  $\text{BCl}_3$  or  $\text{BBr}_3$  before adding to the monomer solution. The goal was to promote the complexation of the borohalide with ether, similar to that of  $\text{BF}_3\text{-OEt}_2$ . However, when adding ether to facilitate co-initiation of PHA, the yield remained zero. The ether does not appear to be playing a role in the polymerization of PHA, other than maintaining the solution concentration of the  $\text{BF}_3$ .

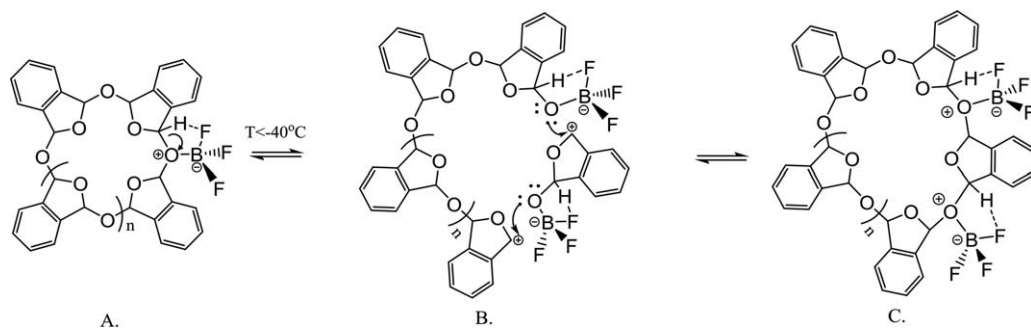
Metal halide and alkyl metal Lewis acids were used to test the catalysis of PHA at different acid strengths. It is noted

that  $\text{ZnCl}_2$  was not soluble in the reaction solution, meaning that if any reaction were to take place, it would need to occur at the unfavorable solid-liquid interface.  $\text{AlEt}_3$  is probably too weak of an acid to polymerize PHA at such low loadings. Yield for the  $\text{TiCl}_4$  polymerization was low (30%) and the polymer was stable for less than 20 days at  $0^\circ\text{C}$ .  $\text{TiF}_4$  did not yield polymer even though its acidity is close to  $\text{BF}_3$ .<sup>23</sup> A possible explanation is that there is a difference in binding energy between the catalyst and the aldehyde. Lewis acidity does not appear to be the sole predictor for PPHA yield.  $\text{BF}_3$  provides the best reaction conditions for stable, high-molecular-weight PPHA.

To elucidate the structure of the intermediates during polymerization, *in situ*  $^1\text{H}$  NMR of the PHA and  $\text{BF}_3\text{-OEt}_2$  reaction was used. An NMR sample in 0.75 mL of  $\text{CD}_2\text{Cl}_2$  was prepared with 5.6 mmol PHA and 1.1 mmol  $\text{BF}_3\text{-OEt}_2$ . An NMR spectrum was obtained at each of five different temperatures,  $-80^\circ\text{C}$ ,  $-65^\circ\text{C}$ ,  $-50^\circ\text{C}$ ,  $-45^\circ\text{C}$ , and  $-42^\circ\text{C}$ . At each temperature, the spectrum was obtained after monomer-polymer equilibrium was obtained, defined as the time when no change in the peak integrals was observed, approximately 15 min at temperature. Figure 1 shows the  $^1\text{H}$  NMR spectra for the five temperatures.

Peaks that can be assigned to the catalyst,  $\text{BF}_3\text{-OEt}_2$ , are shown at 4.2 (d) and 1.35 (c) ppm for the  $-\text{CH}_2-$  and  $-\text{CH}_3$  of the etherate, respectively. Ether ( $-\text{CH}_2-$ , f, 3.42 ppm and  $-\text{CH}_3$ , e, 1.13 ppm) that has become free from the influence of  $\text{BF}_3$  is also shown. The inset focuses on a peak (a, 11.05 ppm) that is shifted further downfield than the monomer peak (aldehyde, 10.45 ppm). This peak is believed to be associated with the free propagating cation, as shown by the chemical structure. A large peak at 6.5 ppm is associated with a polyether proton closely influenced by  $\text{BF}_3$ . The large number of protons that are shifted to 6.5 ppm could show the influence of multiple  $\text{BF}_3$  molecules complexing with the polyether backbone, as shown in Scheme 2(A). The ether protons on either side of the oxygen bound to the boron could be influenced by the cationic oxygen.

As the temperature decreased, the peak at 11.05 ppm decreased, showing a reduced number of cations and propagating chains. The consumption of complexed monomer



**SCHEME 2**  $\text{BF}_3$  complexes with existing polymer backbone (A). Rearrangement and opening of polymer chain (B) allows another monomer to insert itself. Both  $\text{BF}_3$  complexes allow closing of polymer chain (C).

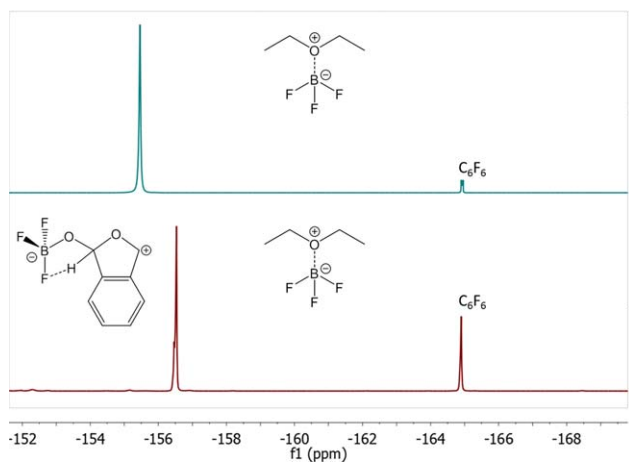


**FIGURE 2**  $^{19}\text{F}$  NMR spectra of  $\text{BF}_3\text{-OEt}_2$  at room temperature (top) and PHA and  $\text{BF}_3\text{-OEt}_2$  mixture at  $-80^\circ\text{C}$  (bottom). [Color figure can be viewed at [wileyonlinelibrary.com](http://wileyonlinelibrary.com)]

during polymerization would cause a reduction of the 11.05 ppm peak. The peak at 6.5 ppm also decreased slightly, possibly from the smaller number of  $\text{BF}_3$  complexed to the polymer. Once quenched, cleaned, and dried, the peaks at 11.05 and 6.5 ppm do not appear in a  $^1\text{H}$  NMR spectrum of PPHA. The  $^1\text{H}$  NMR provides confirmation of the structure that  $\text{BF}_3$  and the aldehyde create when mixed at the reaction conditions necessary to create polymer (i.e., below the ceiling temperature).

There is also additional information concerning the interaction of  $\text{BF}_3$  with monomer and polymer in the peak shifts of the free ether,  $\text{OEt}_2$ . At room temperature, the  $\text{BF}_3\text{-OEt}_2$  structure is a pair of broad peaks at 4.2 and 1.35 ppm. At low temperature, the equilibration between different complexed structures is slowed so that separate NMR peaks are observed with and without  $\text{BF}_3$  interaction.<sup>29</sup> The ether that is not actively complexed with  $\text{BF}_3$  will have peak positions more closely aligned to that of diethyl ether ( $-\text{CH}_2-$ , 3.43 ppm and  $-\text{CH}_3$ , 1.15 ppm). Complexation with ether is likely more favored than complexation with the polyether backbone.<sup>30</sup> As the  $\text{BF}_3$  becomes less involved in the polymerization, it will preferentially return to complexation with  $\text{OEt}_2$ , slightly shifting the ether peaks downfield.<sup>31</sup> This is best seen at the peaks around 3.43 ppm in Figure 1. A decrease in temperature causes the  $-\text{CH}_2-$  peaks of the ether to shift downfield from 3.43 ppm (green) to 3.55 ppm (purple) as a consequence of  $\text{BF}_3$  complexation.

$^{19}\text{F}$  NMR was used to verify the interaction between  $\text{BF}_3$  and the polymer backbone. This is best observed by the peak shifting between  $\text{BF}_3\text{-OEt}_2$  and the complex formed at cold temperatures between  $\text{BF}_3$  and PHA. Two NMR samples were prepared in  $\text{CD}_2\text{Cl}_2$ , one with  $\text{BF}_3\text{-OEt}_2$  and an internal standard of hexafluorobenzene, and another with the same concentration of monomer and catalyst as the  $^1\text{H}$  NMR study and an internal standard of hexafluorobenzene. Figure 2 shows the  $^{19}\text{F}$  NMR spectra at room temperature for

$\text{BF}_3\text{-OEt}_2$  alone (top) and at  $-80^\circ\text{C}$  for the monomer and  $\text{BF}_3\text{-OEt}_2$  solution (bottom). The representative peak for  $\text{BF}_3\text{-OEt}_2$  is  $-154.5$  ppm. Adding PHA and allowing the mixture to cool to  $-80^\circ\text{C}$ , causes the peak to shift upfield to  $-156.5$  ppm. The explanation for the shift is a change in the  $\text{BF}_3$  complexation equilibrium caused by polymerization. A small side peak also appears at  $-156.47$  ppm that could correspond to  $\text{BF}_3$  complexed with PHA.

The catalyst appears to play a more complex role in the polymerization than simply opening and closing insertion sites with the presence of a counter-ion like previous reports suggest.<sup>15</sup> A polymerization with PHA and  $\text{BF}_3\text{-OEt}_2$  probably has two thermodynamic driving forces: creation of a stable polymer chain as determined by the ceiling temperature phenomenon and the complexation of  $\text{BF}_3$  with the aldehyde monomer units or polyether backbone.<sup>30</sup> Scheme 2 is a proposed mechanism for the insertion of additional monomer into a pre-existing polymer chain. The polymer chain complexes with a  $\text{BF}_3$  molecule, as shown in Scheme 2(A). This complexation can promote the rearrangement of  $\text{BF}_3\text{-OEt}_2$  to form a boron anion and carbocation, as previously shown in Scheme 1(C). An additional  $\text{BF}_3$ -monomer complex can insert between the anion and cation of the polymer as shown in Scheme 2(B), conserving charge and allowing for close proximity of the  $\text{BF}_3$  complexes with neighboring carbocations. The  $\text{BF}_3$  complex and carbocation can rearrange back to a closed polymer chain, Scheme 2(C). Rapid exchange of the  $\text{BF}_3$  molecules between free monomer, diethyl ether, and polyether backbone allow further insertion of monomer or oligomer units into the growing polymer chain.

A traditional cationic addition mechanism could provide chain growth until back-biting occurs to allow the  $\text{BF}_3$  complex to close the cyclic polymer chain. An alternate explanation for the  $\text{BF}_3$  catalyzed polymerization of PHA could be that multiple  $\text{BF}_3$ -monomer complexes come together to form an ionically aligned group that allows the  $\text{BF}_3$  rearrangement shown in Scheme 2(C) to close the cyclic polymer chain.

To further probe the role of  $\text{BF}_3$  in the polymerization of PHA, reactions were quenched at various times. Figure 3 shows the yield fraction, molecular weight, and polydispersity index ( $\mathcal{D}$ ) of these reactions. There is little change in molecular weight and yield fraction for the polymerization of PHA catalyzed by  $\text{BF}_3\text{-OEt}_2$ . The shortest reaction time of 15 min seems to be sufficient to reach equilibrium. The  $\mathcal{D}$  may decrease slightly with reaction time supporting the NMR observations.

A fast cationic growth mechanism with rapid initiation and exchange of the active propagation site can explain the high  $\mathcal{D}$  values, as seen for  $\text{BF}_3\text{-OEt}_2$  catalyzed PHA polymerization.<sup>32,33</sup> Yield fraction, molecular weight, and  $\mathcal{D}$  would be expected to be unchanged with time if the Scheme 2 mechanism was true.<sup>15,19,20</sup> The polymer chains quickly mature and reach an asymptotic equilibrium due to the ability of monomer units to be easily removed and inserted. Some of

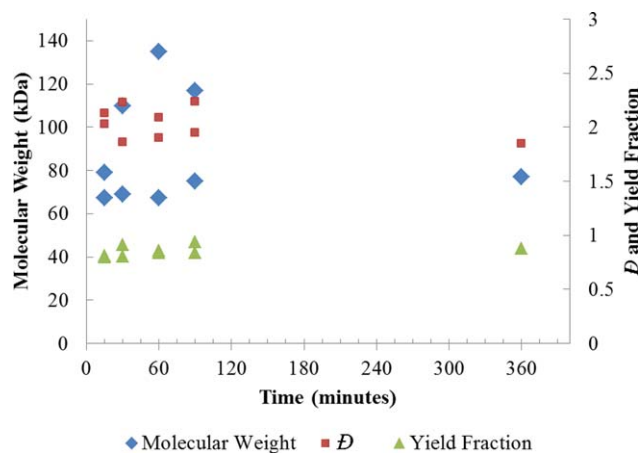


**FIGURE 3** Molecular weight in kDa (diamonds, left axis),  $\bar{D}$  (squares, right axis), and Yield Fraction (triangles, right axis) versus reaction time in minutes of PPHA. [Color figure can be viewed at [wileyonlinelibrary.com](#)]

the differences in the experiments are the amount of catalyst used for the polymerization. In previous studies, much larger quantities of  $\text{BF}_3\text{-OEt}_2$  were used.<sup>14</sup> With a larger amount of  $\text{BF}_3$ , the catalyst could simultaneously interact with multiple locations on the polymer chain, allowing the removal and insertion of oligomers of PPHA, as proposed in Scheme 2.

Multiple polymerizations were performed to determine the effect of catalyst loading on molecular weight. A theoretical molecular weight can be inferred by assuming that each catalyst initiates one chain. Each chain then propagates equally until the monomer is fully consumed. This results in a  $\bar{D}$  of 1.0. Figure 4 shows the molecular weight in kDa versus monomer-to-catalyst ratio for the experimental data (individual points) as well as the theoretical molecular weight from a  $\bar{D}$  of 1.0 (line).

The polymerizations from Figure 4 were re-plotted to show the effective utilization of the monomer. Figure 5 shows the

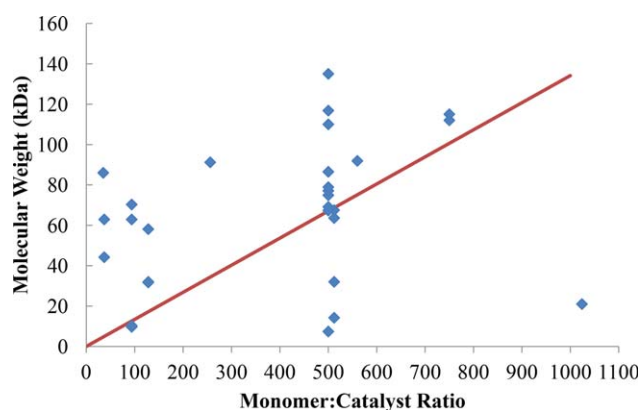


**FIGURE 4** Molecular weight in kDa versus monomer:catalyst (phthalaldehyde: $\text{BF}_3\text{-OEt}_2$ ) ratio. A lower monomer-to-catalyst ratio means larger amounts of catalyst. [Color figure can be viewed at [wileyonlinelibrary.com](#)]

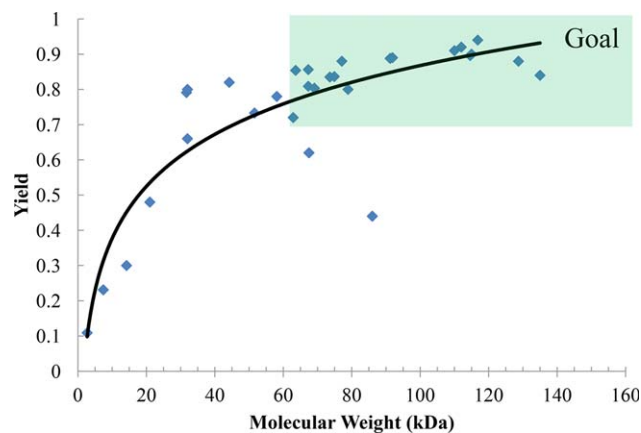


**FIGURE 5** Yield of PPHA polymerizations with  $\text{BF}_3\text{-OEt}_2$  versus molecular weight as determined by GPC in kDa. [Color figure can be viewed at [wileyonlinelibrary.com](#)]

polymerization yield versus molecular weight in kDa. A trend line is shown for ease of viewing. The top right is shaded to show desired polymerization results. The molecular weight increases with monomer utilization. This is expected if the polymerization proceeds with traditional propagation and termination. This also shows a lower and upper limit of the molecular weight of PPHA formed with  $\text{BF}_3\text{-OEt}_2$  catalyst. Low monomer utilization leads to low molecular weight and the upper limit of molecular weight appears capped. A minimum molecular weight is not unreasonable due to the steric strain that could occur in the cyclic polymer. The oligomer must be of a certain size before it can back-bite to form the cyclic polymer. The reproducibility of the polymerization with  $\text{BF}_3\text{-OEt}_2$  catalyst can be seen from the data in Figures 4 and 5. Each data point is a separate reaction. In many cases, there was no intentional change in procedure, although, it is recognized there are minor changes in experimental conditions that occur over a period of months. At low monomer-to-catalyst ratio (i.e., more catalyst), a higher than expected molecular weight is observed. Most of the previously published reports use a low monomer-to-catalyst ratio with  $\text{BF}_3\text{-OEt}_2$  catalyst.<sup>15,19</sup> As the catalyst loading decreased (increasing monomer-to-catalyst ratio), there is considerable scatter in the results. The exact cause of the reaction-to-reaction scatter is still under investigation. This data does show the sensitivity of the reaction to what may be subtle changes in reaction conditions. One such condition, glove box humidity, is known to limit yield by forming a hydrate with the PPHA monomer.

The ambient stability of PPHA has been a major concern for its use and commercialization. Unpredictable depolymerization of PPHA has been common. Some polymers have depolymerized in 6 months, and some have depolymerized within days. Reports of anionic PPHA decomposition suggest a slow loss of material that can be described as 1% depolymerization per day.<sup>6</sup> This could be due to the stability of the end-caps, the likely weakest bonds of the anionic material. The stability of PPHA was studied here by accelerated aging of

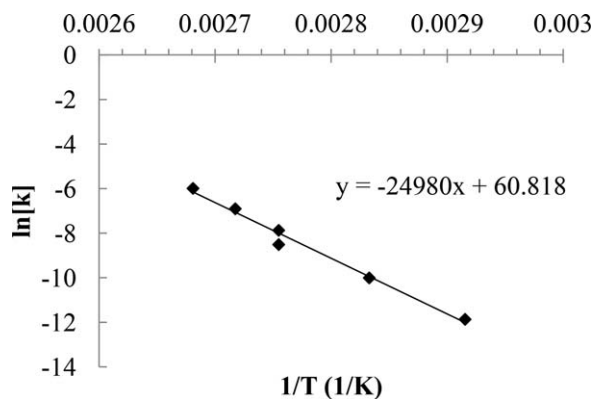


**FIGURE 6** Arrhenius plot for the degradation rate at various isothermals for PPHA.

the  $\text{BF}_3$ -initiated polymers purified by methods reported in literature.<sup>15</sup>

Isothermal gravimetric analysis at 70°C, 80°C, 90°C, 95°C, and 100°C was used to determine the Arrhenius parameters for the depolymerization reaction. The natural log of the mass was plotted versus the time at elevated temperature and linear regression was used to determine the rate of depolymerization at each temperature. The natural log of the rate obtained from the Arrhenius expression at each temperature was plotted versus the reciprocal of temperature, the relationship for first-order kinetics, in Figure 6. A linear regression was used to determine the Arrhenius parameters from these data points. The activation energy was found to be 50 kcal/mol, and the pre-exponential was  $2.6 \times 10^{26}$ .

The activation energy is close to the reported values for the bond strength of an ether C—O bond, which is the expected weakest bond in the PPHA polymer chain.<sup>34</sup> Using these parameters, lifetime estimations were made for PPHA at various temperatures. At 40°C, the polymer would be expected to last 21 days before 1% loss of material occurs. At ambient storage conditions in a laboratory (20°C), the polymer is expected to last 13 years before 1% loss of material. These values for the cationic polymerization are contrary to past experiences and previous reports for the anionic polymerization where ambient temperature shelf-life was much shorter.<sup>6</sup> These results show that  $\text{BF}_3\text{-OEt}_2$  catalyzed PPHA is inherently stable and suggests that an external stimulus is the likely cause of the stochastically observed depolymerization.

Samples of the  $\text{BF}_3\text{-OEt}_2$  catalyzed polymer were sealed in vials to observe the decomposition over time. A transition from a white solid polymer to a transparent solid preceded depolymerization.  $^1\text{H}$  NMR was performed on a polymer that was undergoing depolymerization to try and identify the cause of the depolymerization. The NMR spectrum showed a surprisingly large peak at 6.4 ppm, which corresponds to the  $\text{BF}_3$ -polymer complex. The  $\text{BF}_3$  catalyst was thought to be removed by drying each sample until the mass no longer changed. This was confirmed by  $^1\text{H}$  NMR of the polymer post-drying showing no such peak at 6.4 ppm. However, it

appears that a small quantity of catalyst remained in the polymer. Only after depolymerization began did the peak at 6.4 ppm become apparent. Due to the catalytic nature of the depolymerization of PPHA, aforementioned, a small amount of catalyst remaining in the polymer would be detrimental to its stability. As a consequence of the complex formed between  $\text{BF}_3$  and the polymer backbone, the removal of  $\text{BF}_3$  appears to be difficult and could have led to the stochastic instability previously observed.

To address the issue of residual  $\text{BF}_3$  catalyst, a new purification procedure was developed. Previously, the polymer was purified according to previous reports by redissolving the PPHA in DCM followed by precipitation in hexane.<sup>14,15</sup> The new purification procedure involved solvents with higher binding energies to  $\text{BF}_3$  than the PPHA ether or  $\text{OEt}_2$  to help remove residual  $\text{BF}_3$ . THF, which has a higher binding energy to  $\text{BF}_3$  than diethyl ether and DCM, was used to redissolve the polymer. TEA, which has a higher binding energy to  $\text{BF}_3$  than pyridine, was added to the polymer solution.<sup>30</sup> Finally, the polymer was precipitated and dried as aforementioned. The new purification procedure has provided stable polymer at ambient conditions for months without signs of decomposition. Small samples of PPHA were stored at ambient temperature in sealed vials containing atmospheres saturated with acetic acid (glacial), hydrochloric acid (30–38% in water), *n*-methyl pyrrolidone, pyridine, TEA, THF, water, trifluoroacetic acid, and isopropyl alcohol. Only the vial containing a strong acid, trifluoroacetic acid, resulted in PPHA decomposition, as expected. After 260 days, the date of this manuscript, all other samples remain stable. Low temperature storage should further improve stability during storage.

## CONCLUSIONS

The role of  $\text{BF}_3\text{-OEt}_2$  in the polymerization of high-molecular-weight PPHA was investigated. The Lewis acidity and presence of fluorides for hydrogen bonding appear to make it uniquely suited for PPHA synthesis. A complex interaction of  $\text{BF}_3$  with the monomer and polymer chains was observed by *in situ* NMR. The polymerization time was less than 15 min to reach equilibrium. High molecular weight can be consistently achieved in the polymerization of PPHA by selecting the correct monomer-to-catalyst ratio, which promotes high yield. PPHA in the process of depolymerization showed residual catalyst remained despite traditional purification. An improved method of removing residual catalyst was effective at stabilizing the polymer and improving shelf-life. Accelerated aging of PPHA suggests the polymer is stable for long time periods.

## ACKNOWLEDGMENTS

This work was sponsored by the Defense Advanced Research Project Agency with award W31P4Q-14-C-0118. The authors gratefully acknowledge the help of Leslie Gelbaum in the Georgia Tech NMR Center.

## REFERENCES AND NOTES

- 1 B. Fan, J. F. Trant, A. D. Wong, E. R. Gillies, *J. Am. Chem. Soc.* **2014**, *136*, 10116–10123.
- 2 M. E. Roth, O. Green, S. Gnam, D. Shabat, *Chem. Rev.* **2015**, *116*, 1309–1352.
- 3 S. T. Phillips, J. S. Robbins, A. M. Dilauro, M. G. Olah, *J. Appl. Polym. Sci.* **2014**, *131*, 40992.
- 4 S. T. Phillips, A. M. Dilauro, *ACS Macro Lett.*, **2014**, *3*, 298–304.
- 5 C. W. Park, S. K. Kang, H. L. Hernandez, J. A. Kaitz, D. S. Wie, J. Shin, O. P. Lee, N. R. Sottos, J. S. Moore, J. A. Rogers, S. R. White, *Adv. Mater.*, **2015**, *27*, 3783–3788.
- 6 A. M. DiLauro, S. T. Phillips, *Polym. Chem.*, **2015**, *6*, 3252–3258.
- 7 H. L. Hernandez, S. K. Kang, O. P. Lee, S. W. Hwang, J. A. Kaitz, B. Inci, C. W. Park, S. Chung, N. R. Sottos, J. S. Moore, J. A. Rogers, S. R. White, *Adv. Mater.* **2014**, *26*, 7637–7642.
- 8 E. Uzunlar, J. Schwartz, O. Phillips, P. A. Kohl, *J. Electron. Packag.* **2016**, *138*, 20802.
- 9 L. F. Thompson, M. J. Bowden, *J. Electrochem. Soc.* **1973**, *120*, 1722.
- 10 H. Ito, *Adv. Polym. Sci.* **2005**, *172*, 37–245.
- 11 H. Ito, C. G. Willson, *Polym. Eng. Sci.* **1983**, *23*, 1012–1018.
- 12 A. M. DiLauro, J. S. Robbins, S. T. Phillips, *Macromolecules* **2013**, *46*, 2963–2968.
- 13 M. Tsuda, M. Hata, R. Nishida, S. Oikawa, *J. Polym. Sci. Part A Polym. Chem.* **1997**, *35*, 77–89.
- 14 J. A. Kaitz, C. E. Diesendruck, J. S. Moore, *Macromolecules* **2013**, *46*, 8121–8128.
- 15 J. A. Kaitz, C. E. Diesendruck, J. S. Moore, *J. Am. Chem. Soc.* **2013**, *135*, 12755–12761.
- 16 J. De Winter, A. P. Dove, A. Knoll, P. Gerbaux, P. Dubois, O. Coulembier, *Polym. Chem.* **2014**, *5*, 706.
- 17 J. A. Kaitz, C. E. Diesendruck, J. S. Moore, *Macromolecules* **2014**, *47*, 3603–3607.
- 18 O. P. Lee, H. Lopez Hernandez, J. S. Moore, *ACS Macro Lett.* **2015**, *4*, 665–668.
- 19 C. Aso, S. Tagami, T. Kunitake, *J. Polym. Sci. Part A-1.* **1970**, *8*, 1323–1336.
- 20 C. Aso, S. Tagami, *Macromolecules* **1969**, *3*, 414–419.
- 21 C. Ammann, P. Meier, A. Merbach, *J. Magn. Reson.* **1982**, *46*, 319–321.
- 22 C. Aso, S. Tagami, T. Kunitake, *J. Polym. Sci. Part A-1.* **1969**, *7*, 497–511.
- 23 G. Hilt, F. Pünner, J. Möbus, V. Naseri, M. A. Bohn, *Eur. J. Org. Chem.* **2011**, *30*, 5962–5966.
- 24 P. Laszlo, M. Teston, *J. Am. Chem. Soc.* **1990**, *112*, 8750–8754.
- 25 D. P. N. Satchell, R. S. Satchell, *Chem. Rev.* **1969**, *69*, 251–278.
- 26 E. J. Corey, J. J. Rohde, A. Fischer, M. D. Azimioara, *Tetrahedron Lett.* **1997**, *38*, 33–36.
- 27 A. G. Evans, G. W. Meadows, *Trans. Faraday Soc.* **1950**, *46*, 327–331.
- 28 J. P. Kennedy, S. Y. Huang, S. C. Feinberg, *J. Polym. Sci.* **1977**, *15*, 2801–2819.
- 29 J. J. Gajewski, P. Ngerneemesri, *Org. Lett.* **2000**, *2*, 2813–2815.
- 30 P. C. Maria, J. F. Gal, *J. Phys. Chem.* **1985**, *89*, 1296–1304.
- 31 B. Y. R. A. Craig, R. E. Richards, *Trans. Faraday Soc.* **1963**, *59*, 1962–1971.
- 32 C. Yuan, D. Yan, *Makromol. Chem.* **1987**, *188*, 341–348.
- 33 C. Yuan, D. Yan, *Polym. J.* **1988**, *29*, 924–928.
- 34 W. van Scheppingen, E. Dorrestijn, I. Arends, P. Mulder, H. G. Korth, *J. Phys. Chem. A* **1997**, *101*, 5405–5411.